JOURNAL OF MATERIALS SCIENCE 33 (1998) 887–894

Lattice dynamics of colloidal crystals during photopolymerization of acrylic monomer matrix

H. B. SUNKARA*[+], B. G. PENN[‡], D. O. FRAZIER[‡], N. RAMACHANDRAN[‡§]
*Du Pont Nylon, Polymer Science and Engineering Technology Center, Experimental Station, PO Box 80302, Wilmington, DE 19880, USA
E-mail: Hari.B.Sunkara@USA.DUPONT.COM
[‡]NASA Marshall Space Flight Center, Space Sciences Laboratory, Huntsville, AL 35812, USA

The photoinitiated bulk polymerization process, which has been used recently in the manufacture of solid optical diffraction filters, is examined to understand the dynamics of both the crystalline colloidal arrays (CCA) and the host monomer species. Our analysis indicates that volume shrinkage of the monomer, changes in the dielectric properties of the monomer, and inhomogeneities of polymerization reaction rate across the dispersion during the polymerization process, are the major contributors for observed lattice compression and lattice disorder of the CCA of silica spheres in polymerized acrylic/methacrylic ester films. The effect of orientation of photocell with respect to the radiation source on Bragg diffraction of CCA indicated the presence of convective stirring in the thin fluid system during the photopolymerization that deleteriously affects the periodic array structures. To devise reproducible and more efficient optical filters, experimental methods to minimize or eliminate convective instabilities in monomeric dispersions during polymerization are suggested.

1. Introduction

Most recently, a unique class of polymer composite thin films, possessing optical diffraction capabilities, has been developed by photoinitiated free radical bulk/solution polymerization of monomeric dispersions in which submicrometre polymer spheres self-assemble into either body- or face-centred cubic structures [1–14]. This class of photonic crystalline materials is finding applications in optical technology as fixed or tunable laser filters, optical switches and optical limiters [8, 14]. One of the primary goals in fabricating these polymer composite filters is to enhance the stability of the colloidal crystals, which when suspended in a liquid medium are very fragile, unstable and extremely sensitive to ionic impurities. The high fragility of crystalline colloidal arrays (CCA) in liquids is due to their very low bulk and shear moduli, and therefore, any bulk fluid motion tends to distort or melt these crystals. Relatively stable colloidal crystals in an aqueous medium can be obtained by using polymer spheres having very stable and high number density of charged surface functional groups [15]. Nonetheless, these colloidal crystals deform when exposed to weak external forces such as gravitational acceleration [16, 17], heat, shear [18] and electric fields [19]. It is a challenging task to convert these delicate and extremely sensitive periodic array structures into highly robust arrays.

The newly developed photopolymerization methodology, which locks-in the macroscopic ordered structures in solid polymer matrices, is fairly successful in overcoming the aforementioned problems. However, the composites face other problems such as lattice compression, lattice disorderness, optical heterogeneities within a single film, scattering losses at wavelengths other than the Bragg regime, and lack of reproducibility. At the present time, the development of these polymer composites is in its infancy, and is more of an art than science. The following issues have to be addressed in order to take the critical step towards the manufacture of efficient diffraction CCA filters from the realm of experimental laboratory work to a developed and mature commercial concept:

(1) understanding the dynamics of CCA and host monomer matrix during the photopolymerization process;

(2) identification of forces that tend to deform colloidal crystals and the elimination or minimization of such forces during polymerization;

(3) understanding the effects of ordered arrays of spheres on polymerization kinetics, and on the microstructure of the polymer matrix and its properties.

On the basis of our previous study, the purpose of this paper is to obtain new physical insights into the process of *in situ* photopolymerization of acrylic monomer matrix in the presence of CCA. This

[+]National Research Council Fellow to whom correspondence should be addressed.
[§]University Space Research Association.

knowledge is essential to the understanding of the observed disparities in the optical diffraction properties between the liquid CCA suspension and the solidified CCA films. We propose a model that explains the experimentally observed lattice compression and lattice disorder during polymerization, and suggest methods for the production of reproducible and more efficient optical filters.

2. Polymer composite films/hydrogel membranes

A variety of polymer composites embedded with CCA has been prepared in the last couple of years [1–14]. These materials are classified into two categories: polymer composite films, and hydrogel composite membranes. The most widely used colloidal spheres in these optical filters are either inorganic silica or organic polystyrene latexes. Before discussing the factors that could affect the optical properties of CCA in polymerized films, we describe briefly the typical experimental procedures used to prepare these composite materials.

2.1. Acrylic polymer composite films

These solid plastic or rubbery thin films are obtained from the bulk photopolymerization of arrays of colloidal silica (surface functionalized with 3-(trimethoxy) silylpropyl methacrylate groups, TPM) suspended in neat acrylic monomers such as methyl acrylate (MA), methyl methacrylate (MMA) or a monomer mixture of MMA/HEMA (hydroxyethyl methacrylate) [1–6]. A typical photopolymerization recipe for silica–PMMA nanocomposite is given in Table I. The photochemical cells that contain the silica dispersions are made of standard microscope glass slides with dimensions 3 in. × 1 in. × 0.1 cm (~7.62 cm × 2.54 cm × 0.1 cm). Two such slides are glued together with a spacer of the desired thickness to make a photocell container. The glass containers are silylated to avoid leaching of ionic species into the dispersion, and to obtain uniform wetting of the surfaces by the non-polar monomeric dispersion. A 450 W medium pressure mercury arc lamp is used as the radiation source. The monomeric dispersions containing a photoinitiator (2,2-dimethoxy-2-phenyl acetophenone, DMPA) are injected into the cell containers and crystallites are grown at room temperature. The *in situ* photopolymerization of MMA or MA dispersions having 35–40 wt % silica, results in glassy or elastomeric composite films in which the TPM–silica spheres are covalently attached to the host polymer chains.

2.2. Acrylamide hydrogel composite membrane

A typical recipe for the preparation of a hydrogel membrane embedded with arrays of polystyrene (PS) latex spheres is also given in Table I [10]. The hydrogels are obtained by exposing quartz cells containing an aqueous dispersion of latex spheres, acrylamide (AM), *N*, *N*′-methylenebisacrylamide (MBA, cross-linker) and benzoin methyl ether (BME, photoinitiator) to ultraviolet light (15W BlackRay Longwave). Upon completion of the polymerization, the CCA of PS latex spheres are trapped in a highly porous cross-linked gel network. In contrast to solid, rigid silica–PMMA films, the PS–PAM gel membranes are semi-solid, fragile and are filled with water by as much as 75% by weight.

3. Optical properties of solidified CCA structures

The issue of major concern in creating optical polymer composite films/membranes for either linear or non-linear optical device fabrication [8, 14] is the lack of reproducibility of optical diffraction properties either from one polymerized film to another or from the polymerized film to its corresponding prepolymerized fluid medium. For example, the optical diffraction properties of solidified CCA of silica spheres in a PMMA matrix significantly differ from the unpolymerized liquid MMA dispersion, as shown in Fig. 1 [1, 3]. A very large shift of the Bragg diffraction peak with a much wider bandwidth is obvious for the polymerized film. The diffraction wavelength is shifted from 554 nm to 490 nm during the polymerization which corresponds to a 15% decrease in the lattice *d*-spacing. The peak bandwidth is found to increase from 4 nm to about 15–20 nm in the polymerized film. A lack of uniformity of the optical properties within a polymerized film has also been observed. In like manner, in the preparation of solidified CCA of polystyrene spheres in polyacrylamide gel matrices, shifting, splitting or disappearance of diffraction peaks has been observed; however, no scientific reasoning has been given for these occurrences [10].

TABLE I Photopolymerization recipes of polymer composite film/membrane

Bulk polymerization[a]		Solution polymerization[b]	
TPM silica spheres (D = 153 nm)	35.0 wt %	Polystyrene latex (D = 109 nm)	8.5 wt %
Methyl methacrylate	65.0 wt %	AM/MBA	3.3 wt %
Photoinitiator (DMPA) [c]	1.0 wt %	Photoinitiator (BME)[c]	0.01 wt %
Reaction time	4.0 h	Sucrose	9.6 wt %
		Solvent (water)	78.6 wt %
		Reaction time	10.0 min

[a] [1].
[b] Example 5 in [10].
[c] Amount of photoinitiator is based upon the total weight of the monomer(s).

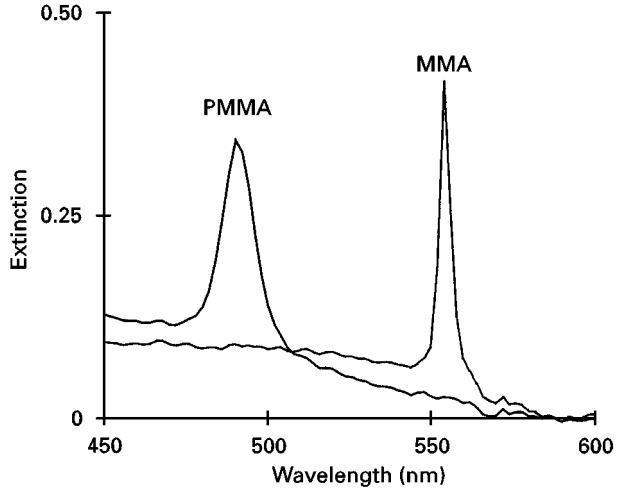

Figure 1 Bragg diffraction from arrays of silica spheres in methyl methacrylate before and after polymerization. The experimental conditions are reported in Table I (see [1]).

TABLE II Properties of polymer spheres, monomer and polymer matrices. The values in parenthesis are temperature in Celcius.

	Density ($g\ cm^{-3}$)	Viscosity (cP)	Dielectric constant (1 MHz)
TPM silica	1.795		
MMA[a]	0.937 (25)	0.54 (25)	6.32[b] (30)
PMMA	1.19		2.60[c] (25)
HEMA[d]	1.070 (25)	5.90 (30)	
Polystyrene	1.05		
Water[e]	0.998 (20)	1.002 (20)	78.5 (25)
Water + 9.5 wt% sucrose[e]	1.036 (20)	1.32 (20)	
Acrylamide	1.122 (30)		
Polyacrylamide	1.302		

[a] [39].
[b] See [38].
[c] [40]
[d] [41]
[e] [42].

In the case of silica–polyacrylic films, the lattice compression causing the observed shift in the diffraction wavelength has been attributed mostly to the volume shrinkage of the host matrix. Based on the experimental observation that only the thickness (but not length and width) of the polymerized film decreases, it has been proposed that the crystalline structure transforms from a face-centred cube to a rhombohedral during the photopolymerization process [5]. Attempts have been made recently to see crystalline structures in solidified PMA films using scanning electron microscopy and ultra-small-angle X-ray diffraction techniques [6].

This model raises the following question: why does the volume of the monomeric dispersion decrease only in thickness during polymerization? For example, the volume fraction of MMA used in the dispersion is 0.805 and hence a 17% decrease in volume (21% for neat MMA) can be expected after polymerization. Because the volume change of the monomer matrix occurs at the molecular level, the volume should shrink uniformly in all three dimensions with a 5.6% decrease in each dimension. Experimental observations have shown a profound decrease in the host volume of the polymerized film only in one dimension, the thickness by about 14% [5]. Obviously, this non-uniform matrix shrinkage deforms the lattice structures. The above model does not take into account the interparticle interaction of spheres which can affect the lattice dynamics of colloidal crystals. It is known that the polymer spheres in the lattice vibrate continuously from their equilibrium positions, and colloidal crystals dynamically respond to an external radiation stimulus [20–23].

4. Factors affecting the periodic arrays during polymerization

Besides the matrix volume, the changes in dielectric properties of the matrix during the photopolymerization of silica–MMA dispersions also affect the dynamics of colloidal crystals particularly in the initial stages of the reaction. Our rationale behind this prediction is as follows: as the monomer converts to polymer, the dielectric constant of the host medium decreases for two reasons. Firstly, the polarizability of vinyl monomer is greater than the monomer unit in the corresponding polymer (the dielectric constants of MMA and PMMA are listed in Table II), and secondly the dielectric constant of the monomer is temperature dependent. An increase in temperature due to an exothermic reaction can decrease the dielectric constant of the reacted species. This decrease in dielectric constant of the host decreases the electrostatic repulsive interaction between the spheres as a result of counter-ion association. The reduced interparticle interaction drives the colloidal crystals to shrink during polymerization. Equation 1 shows the dependency of interparticle interaction potential, U, between two spheres of radius a at a distance r on the dielectric constant, ε, of the medium [20]

$$U(r) = \frac{(Ze)^2}{\varepsilon}\left[\frac{\exp(ka)}{1+ka}\right]^2 \frac{\exp(-kr)}{r} \qquad (1)$$

where Ze is the particle charge (Z is the number of charges per sphere and e is the electronic charge), and the inverse Debye screening length k is given by

$$k^2 = \frac{4\pi e^2}{\varepsilon k_B T}(n_p Z + n_i) \qquad (2)$$

where n_p is the particle concentration, n_i is the ionic impurity concentration, k_B is the Boltzmann constant and T is the temperature.

The effect of polarizability of dielectric medium on colloidal crystals of TPM silica has been demonstrated by Phillipse and Vrij [24]. The number of charges, Z, on a TPM silica sphere was found to decrease from $\sim$500 to 90 as the dielectric constant of the medium was changed from a pure ethanol ($\varepsilon = 25$) to a mixture of toluene/ethanol, 70/30 vol/vol ($\varepsilon = 10$). As a result of decrease in sphere charge, the inverse Debye length, k, decreased from 100 nm to about 50 nm. In another study, the effect of local heating of colloidal crystals suspended in an aqueous medium using a laser beam on lattice compression, has been

investigated by Rundquist *et al.* [20, 21]. The localized compression of the dyed colloidal crystals has been attributed to reduced electrostatic interaction between the spheres, which results from the temperature-dependent dielectric constant of the water medium. They observed no changes in the crystalline structure during the lattice compression, and found time scales of such lattice compressions to be of the order of few seconds. These experiments clearly support our assumption that the change in dielectric constant of the matrix is also responsible for the lattice shrinkage during the polymerization at initial stages, and any inhomogeneities in dielectric properties in the dispersion can cause lattice disorder (see the following section). At later stages of the reaction, the rapid increase in fluid viscosity prevents the collective diffusion of colloidal crystals.

The other factor which can affect the CCA during the polymerization is gravity-driven convective stirring in the dispersion. It is well known that gravity-induced convective flows arise in an unstirred system whenever density gradients are present [25]. There are several variations that can create density gradients: the presence of more than one phase, material phase transition from one state to another, and differences in either temperature or concentration in the system. Evidence of convective stirring has been reported recently during the photopolymerization of bulk systems like acrylamide [26, 27], methyl methacrylate [28], and as well as in the formation of polydiacetylene thin films from the bulk monomer solution phase [29, 30]. Such shear convective flows could easily distort or melt the delicate and fragile CCA. However, it should be pointed out that most of the convective effects in the polymerization process are manifest within the first 25% of the total conversion of monomer into polymer. This is due to the onset of the Trommsdorff gel effect, typical of the bulk MMA polymerization process [31], which essentially freezes the inner structures with a rather abrupt viscosity increase at the transition point. Before arguing the effect of convection on organized colloidal spheres during the polymerization process, we discuss the origins of convection in colloidal dispersions, and the factors that most influence these convective flows.

4.1. Origins of convective instabilities in silica–MMA dispersions

As the ultraviolet radiation penetrates into a monomeric dispersion, the light attenuates gradually in the direction of propagation due to absorption of light by the photoinitiator and the monomer molecules present in the dispersion. The concentration of the photoinitiator, DMPA (the molar absorption coefficient at 336 nm = 274 $cm^{-1}\,mol^{-1}\,l$), employed in a 0.26 mm thick dispersion is 1 wt % based on the monomer weight (Table I). If both the initiator concentration and its molar extinction coefficient are high in the dispersion, this can lead to large intensity gradients, resulting in large buoyancy forces and convection. The self-screening effect by the photoinitiator molecules cannot be eliminated but may be reduced by carefully choosing an optimum concentration of photoinitiator for a given thickness of the dispersion [32].

The incident light is also attenuated due to scattering by the colloidal silica spheres and the grain boundaries of polycrystalline domains present in the monomer matrix. The silica spheres are 150 nm in diameter which are stacked with hexagonal close-packed planes and occupy about 20% of the total volume. The turbidity which is a measure of scattering by the spheres in the dispersion can be represented as [8, 33]

$$\tau = (2.303)\, Nb\pi r^2 Q_{\text{ext}} \tag{3}$$

$$Q_{\text{ext}} = \frac{32}{27}\left(\frac{n_s}{n_m} - 1\right)^2 \left(\frac{2\pi r}{\lambda}\right)^4 \tag{4}$$

where b is the path length, r is the particle radius, N is the number density of spheres, Q_{ext} is the scattering efficiency, n_s and n_m are the refractive indices of particle and medium, respectively. The above equations indicate that the scattering is a strong function of particle size (sixth power), wavelength (inverse fourth power) of light and of contrast in the refractive index. The intensity losses due to absorption and scattering result in an intensity gradient along the direction of light propagation in the dispersion. Because of this intensity gradient in the dispersion, the polymerization rate, R_p, which is intensity I_o dependent [34] as shown in Equation 5, varies in the dispersion. Hence, the reaction rate would be faster at the dispersion layers where the light enters and would decrease gradually in the medium

$$R_p = \frac{k_p}{(k_t)^2}\,[M][\varphi I_o(1 - 10^{-\beta c_i b})] \tag{5}$$

where k_p and k_t are the rate constants of propagation and termination, $[M]$ and c_i are the monomer and initiator concentrations, ϕ is the quantum yield, and β is molar absorption coefficient of the photoinitiator.

Further, because the addition polymerization reaction is exothermic (the heat of polymerization of MMA is 13.4 kcal mol^{-1} with an adiabatic temperature rise of ~250 °C), the liberated heat causes a thermal gradient in the dispersion due to lack of thermodynamic equilibrium. Additionally, the glass cells used to fill the colloidal array dispersions can also absorb the ultraviolet radiation and cause thermal gradients in the dispersion. These thermal gradients in the dispersion generate density gradients ($\Delta\rho_{\text{thermal}}$ is negative), and the density gradients under the influence of gravity can induce convective fluid motion. There is little experimental evidence in the literature that reveals the presence of thermally driven convective motion in colloidal dispersions [21, 35]. Melting of colloidal crystals of dyed PS spheres suspended in an aqueous medium has been observed when the local temperature of the dispersion was increased by an intense laser beam [21]. Recently, Thies-Weesie and Philipse [35] have also demonstrated that light- induced convection can disturb the sedimentation process of colloidal particles. A small rise in temperature (≈ 0.3 °C) in the dispersion due to the absorption of light by light-absorbing colloidal silica–haematite prolate particles dispersed in an organic solvent,

caused large-scale convection. However, no similar convection was observed when silica spheres (without the haematite pigment) were used. In our polymerization experiments, the temperature rise due to the absorption and exothermicity could give rise to such bulk convection in the system.

Another factor that can cause bulk convection in addition to a thermal gradient, is changes in the composition (solutal gradient). The large decrease in partial molar volume, ΔV, of the host MMA medium during polymerization can give rise to a density gradient in the dispersion ($\Delta\rho = \rho_{polymer} - \rho_{monomer} = 0.25\,g\,cm^{-3}$, Table II). This decrease in volume is due to conversion of van der Waals distances between atoms to covalent bond distances. The net density change during the polymerization of monomeric dispersion can be written as

$$\Delta\rho = \Delta\rho_{thermal} + \Delta\rho_{solutal} \quad (6)$$

It is to be noted in Equation 6 that $\Delta\rho_{thermal}$ is of opposite sign with respect to $\Delta\rho_{solutal}$.

It is very clear from the above arguments that a large density gradient can arise during the photopolymerization of CCA dispersion in thin containers and the following experimental results strongly support the presence of convective forces.

Orientation effects of the photocell. *In situ* polymerization of silica–MMA dispersions in photochemical cells which are kept in the horizontal position rather than vertical (as shown in Fig. 2) has led to composite films which Bragg diffract the incident light in a way similar to liquid dispersions [1]. The composite films obtained in the vertical orientation with side ultraviolet illumination, however, showed no Bragg diffraction (Fig. 2a). This dramatic effect of orientation of the photocell with respect to the gravity vector, on the ordered arrays of TPM silica spheres suspended in MMA, suggests the presence of convection in the thin cells. Because no other experimental parameter, other than the cell orientation, was changed, and neither the heat of polymerization nor the properties associated with volume shrinkage of the host are affected by geometric considerations, the observed phenomenon can only be attributed directly to gravity effects. The explanation for the observed optical diffraction from the cells which were irradiated from the top (horizontal orientation) and those subjected to sidewise irradiation (vertical orientation) is now presented.

The disappearance of Bragg diffraction from solidified films is a result of either the complete destruction of ordered arrays of spheres or due to the disorientation of the lattice planes of the crystallites. For example, in the face-centred cubic (fcc) crystallites, the most dense $d_{(1\,1\,1)}$ planes on average orientationally align themselves parallel to the surface of the photocell. Crandall and Williams [16], and Kesavamoorthy and Arora [17] have observed that the gravitational force significantly affects the interacting colloidal polystyrene spheres (100 nm diameter and density of $1.05\,g\,cm^{-3}$) dispersed in an aqueous medium resulting in a lattice compression at the bottom of the container. Therefore, our initial reasoning for the disappearance of the Bragg diffraction peak

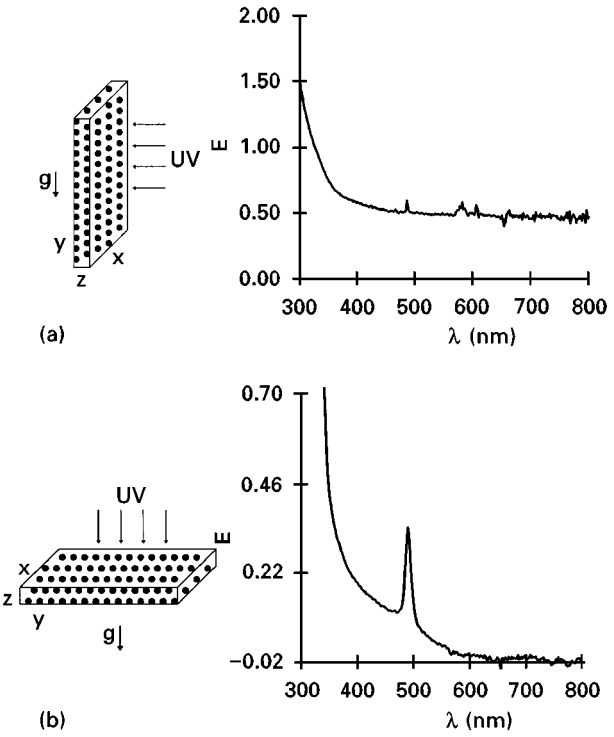

Figure 2 The effect of orientation of the photocell with respect to radiation source on optical properties of silica–PMMA composites. (a) Vertical orientation of the photocell containing the dispersion and ultraviolet light incident from the side. The extinction, *E*, spectrum of polymerized film shows the absence of the Bragg diffraction peak present in the MMA matrix before polymerization. (b) Horizontal orientation of the photocell which receives ultraviolet light from the top. The extinction spectrum shows the resulting polymerized film possessing a Bragg diffraction peak. Before polymerizing the dispersions, the photocells were kept in the horizontal position to grow the crystallites for few days. The *x*, *y* and *z* dimensions of the cell are 20, 70, 0.264 mm, respectively.

from the silica–PMMA dispersion, which was kept in the vertical position just before polymerization, was the effect of gravitational force on colloidal crystals. The crystallites of silica spheres, which were grown in an MMA matrix for a few days in the cell kept in the horizontal position, are in gravitational equilibrium, because the rate of sedimentation of spheres is faster than the rate of crystallization [17]. Upon tilting the cell to the vertical position, these crystallites under the influence of gravity tend to reach a new sedimentation equilibrium, and in the process can deform. However, in the experiment, continuous monitoring showed that the Bragg diffraction peak was not destroyed in the unpolymerized dispersion, although the peak position and shape changed, when the fluid sample was held vertically in a spectrophotometer for 3–4 h, the typical duration of the photopolymerization process. These experimental results suggest that the absence of the diffraction peak from the vertically held polymerized sample is not due to the effect of gravitational force on the interacting colloidal spheres but due to enhanced local stirring (causing CCA deformation) caused by convective effects.

It appears that the polymerization process induces more fluid instability in a vertically oriented photocell than that in the horizontal. The effect of instabilities in vertical and horizontal orientations of the photocell with respect to the ultraviolet light is schematically

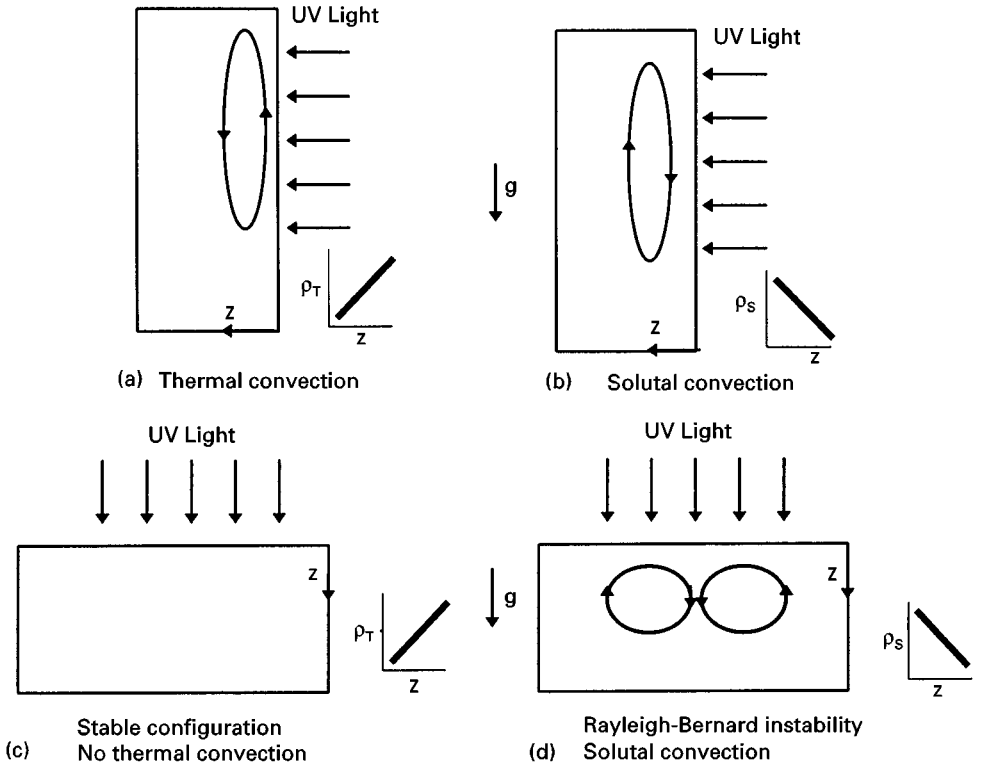

Figure 3 Schematic representation of convective patterns due to thermal, ρ_T, and solutal, ρ_S, gradients that arise in a system during photopolymerization. (a,b) Vertical orientation (radiation incident from the side) of photocells; (c,d) horizontal orientation (radiation incidents from the top). z is the fluid thickness.

represented in Fig. 3. The gravitational force is vertical and acting downward. In both orientations, as was previously discussed, the intensity gradients in the dispersion cause reaction rates to be fastest in dispersion layers closest to the radiation. In the vertical orientation, the fluid layers closer to the radiation source become lighter due to the absorbed radiation and liberated heat, and gravity induces motion of these layers in the upward direction. These layers, however, become denser if a solutal gradient dominates instead of thermal, and again, in this case, gravity drives descending motion of fluid layers. The density changes due to thermal and/or solutal effects cause the immediate onset of convection (thresholdless) in the vertical configuration because the system is unstable and the fluid motion tends to randomize the CCA during polymerization. These different convective motions are sketched in Fig. 3a and b. In reality, the thermal and the solutal effects act together simultaneously in opposite directions and can create a zero net density difference if their magnitudes are equal. Nonetheless, in order to achieve a zero net density difference, a significant thermal gradient is required (typically 100 times larger than the solutal gradient) [36]. This is due to the vast disparity between the diffusivities of heat and mass (heat diffuses faster than mass). Even if the net density change is zero, in systems where thermal and solutal are of opposite signs, convection can still occur due to inherent system instabilities associated with large volume changes of the host monomer, as pointed out by Pojman and Epstein [36]. This fluid convection is usually referred to as double diffusive convection or multicomponent convection.

In the case of the horizontal configuration, however, the heated and therefore less-dense fluid layers are on top (Fig. 3c), over denser bottom layers leading to a stably stratified system. In this instance, gravity does not induce any convection. However, if compositional changes in the system dominate, the top layers become denser than the bottom, leading to Rayleigh–Bernard instability of an interphase surface. In such circumstances, the convective flow pattern shown in Fig. 3d arises only after crossing a critical Rayleigh value. Because the composite film, obtained by polymerizing the dispersion in a horizontally oriented cell (Fig. 2b), Bragg diffracts the incident light, indicating that the critical *Ra* value is perhaps not exceeded, which may be due to the capillary dimensions of the cell. Although there is no bulk convective flow which can melt CCA, the sedimentation of top denser layers can be responsible for the observed lattice disorder (wider Bragg diffraction peaks), decrease in film thickness and local inhomogeneities within the polymerized film.

To assess the most dominant field effect on CCA, we have estimated the thermal Rayleigh number, *Ra* which gives the ratio of free energy liberated by buoyancy to the energy dissipated by heat conduction, and Prandtl number, *Pr*, which is a measure of the relative importance of momentum diffusion to heat diffusion for neat MMA using the following equation

$$Ra = \left(\frac{g\Delta\rho L^3}{\eta\alpha}\right) \tag{7a}$$

$$Pr = (\nu/\alpha) \tag{7b}$$

where L is the characteristic length scale of the system, η and ν are the absolute (dynamic) and kinematic

viscosities of the liquid, and α is the thermal diffusivity ($k/\rho Cp$) where k is the thermal conductivity and Cp is the specific heat. The Rayleigh number for solutal convection is obtained by replacing the thermal diffusivity, α, with solutal diffusivity, D in Equation 7. The v/D term is called the Schmidt number, Sc, which is the solutal analogue of the Prandtl number. In Table III, the estimated thermal and solutal numbers for neat MMA are listed. Much larger solutal Rayleigh and Schmidt numbers than thermal Rayleigh and Prandtl numbers clearly imply that the solutal field most likely dominates any convection within the cell. Therefore, radiating the dispersion from the bottom of the container rather than from the top, could suppress the solutal field instability and can result in films with superior optical diffraction properties if thermal convection is insignificant.

In another experiment, Bragg diffraction has been observed from solidified CCA in poly(MMA-*co*-HEMA) film, in spite of keeping the photochemical cell in a vertical position (Fig. 4) [3]. As stated earlier, the vertical configuration is highly unstable because of buoyancy-induced fluid motion. Such motion, in general, is opposed by viscous drag forces as shown in Equation 8,

$$V = \mathrm{O}\left[\frac{g\Delta\rho L^2}{\eta}\right] = \mathrm{O}[RaPr^{-1}(v/L)] \qquad (8)$$

The O [ ] notation in Equation 8 indicates an order of magnitude estimate of the velocity, V. HEMA is more viscous and denser than MMA (Table II). Therefore, the bulk viscosity of the monomer mixture (MMA/HEMA; 65/35 wt %) is higher than neat MMA, and this highly viscous matrix stabilizes the dispersion against convection. As a result, the periodic arrays of silica spheres are not disturbed completely after polymerization. However, the crystalline lattice is still compressed in this film as observed in PMMA film, and this compression, as explained before, is due to the changes in volume and dielectric properties of the matrix during the polymerization.

TABLE III Estimates of convective parameters for MMA[a]

Rayleigh number, *Ra* (thermal)	230
Rayleigh number, *Ra* (solutal)	83000
Prandtl number, *Pr* (thermal)	7.2
Schmidt number, *Sc* (solutal)	580

[a] The numbers are calculated from Equation 7 choosing the thickness of the photocell (0.264 mm) as the characteristic length, L.

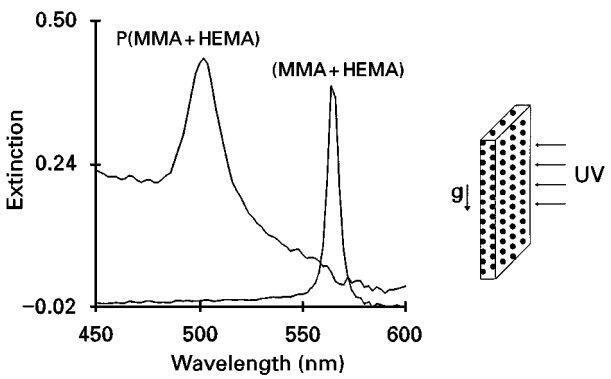

Figure 4 Bragg diffraction from the arrays of silica in a mixture of MMA and HEMA (65/35 wt %) before and after polymerization. The photocell containing the dispersion is tilted vertically just before irradiating the sample from the side.

4.2. Hydrogel composite membrane

The recipe reported in Table I has been used to produce a composite membrane which has optical diffraction properties exactly identical in all aspects to that of its liquid analogue (see Fig. 5 in [10]). We might say that the solution photopolymerization of this recipe is free from convection, because the factors which induce buoyant force during the bulk polymerization of silica-MMA dispersions, such as radiation source intensity, density differences between the spheres and the host, sphere size and number density, concentration of monomer and photoinitiator, viscosity of the fluid, orientation of the photocell with respect to radiation source, and changes in temperature and composition in the system, are not notable. In the following paragraph, the experimental parameters for acrylamide polymerization are examined and compared with respect to MMA polymerization to see how the above factors have insignificant effects on CCA.

The power of the ultraviolet light used to polymerize acrylamide dispersion is only 15 W, which is much lower than the 450 W mercury arc used to polymerize MMA dispersion. Low output intensity, relatively smaller size and low concentration of PS spheres, and very low photoinitiator concentration cause low intensity gradients in the dispersion (Table I). The amount of monomer mixture (90%AM + 10%MBA) used is 3.0 vol % which is indeed very small compared to 80.0 vol % MMA. Highly diluted concentration of acrylamide can produce minimal thermal gradients in the system during the photopolymerization. The volume shrinkage of the monomer mixture during the polymerization is less than 0.5% as opposed to 17% for MMA. Hence, there is minimal solutal convection in the dispersion due to insignificant volume changes of the host matrix. Besides, the large amount of sucrose in the dispersion, which can function as a thickening agent, increases the bulk viscosity of the dispersion (Table II), and therefore, opposes any convective motion. The small difference in densities between the PS spheres and the host medium, the higher viscosity of the matrix, and faster rates of polymerization, prevent any sedimentation as observed with silica–MMA dispersion. Further, the negligible changes in dielectric properties of the host matrix during the polymerization process cause no lattice compression. This experiment offers strong evidence to our proposed model for silica–MMA system. Although the recipe produces an excellent optical filter membrane that fully retains the ordered arrays of PS spheres in liquid dispersion, the major drawback is that the resulting composite membrane is too fragile (low mechanical strength) to be handled for practical applications.

On the other hand, experiments with recipes other than the one mentioned above have resulted in membranes with varied optical diffraction properties [10]. For example, no diffraction was observed from the polymerized sample which contained 20 wt % acrylamide

and no cross-linking comonomer. We attribute the total loss of optical diffraction properties after polymerization entirely to convective stirring arising from buoyancy-driven forces. The high concentration of monomer generates thermal and solutal convections in the system. Acrylamide is more reactive and exothermic (the heat of polymerization is 18.9 kcal mol^{-1}) than the MMA. In thermally initiated AM polymerization, the observed fluid velocities are about one order of magnitude higher than in methacrylic acid polymerization [37]. Gravity-driven macroscopic fluid motions have been observed by Russian researchers [26, 27] during the synthesis of cross-linked PAM gels when samples were irradiated in 3 and 10 mm path length quartz cells. These experimental results indicate that convective motion during the reaction is responsible for the disappearance of Bragg diffraction.

5. Conclusion

We have identified several factors which influence the dynamics of colloidal crystals of silica spheres during the photoinitiated bulk polymerization of an acrylic monomer matrix. The observed discrepancies in the optical diffraction properties of CCA dispersed in solid polymer matrices are reviewed and the factors responsible for these discrepancies are described. The origins of several convective instabilities in the CCA dispersions are discussed and the key role of gravity-induced convective stirring on periodic arrays is demonstrated. In order to manufacture composite films that must retain the liquid crystalline ordered structures, polymerization rate across the dispersion should be uniform, and the matrix volume shrinkage is to be minimized. Microgravity provides a unique convection-free and sedimentation-free quiescent environment that can be used to perform studies that-will lead to a more complete understanding of the photopolymerization process of organized systems.

Acknowledgements

Hari Sunkara thanks the National Research Council for the fellowship and Warren T. Ford for his comments on this paper.

References

1. H. B. SUNKARA, J. M. JETHMALANI and W. T. FORD, *Chem. Mater.* **6** (1994) 362.
2. *Idem*, *ACS Polym. Mater. Sci. Engng Preprint* **70** (1994) 274.
3. *Idem*, in "Hybrid Organic-Inorganic Composites", edited by J. E. Mark, C. Y-C. Lee and P. A. Bianconi, *ACS Symp. Ser.* **585** (1995) 181.
4. J. M. JETHMALANI, H. B. SUNKARA, W. T. FORD, S. L. WILLOUGHBY and B. J. ACKERSON, *Langmuir* **13** (1997) 2633.
5. J. M. JETHMALANI and W. T. FORD, *Chem. Mater.* **8** (1996) 2138.
6. J. M. JETHMALANI, W. T. FORD and G. BEAUCAGE, *Langmuir* **13** (1997) 3338.
7. H. B. SUNKARA, J. M. WEISSMAN, B. G. PENN, D. O. FRAZIER and S. A. ASHER, *ACS Polym. Preprint* **37** (1996) 53.
8. J. M. WEISSMAN, H. B. SUNKARA, A. S. TSE and S. A. ASHER, *Science* **274** (1996) 959.
9. G. HAACKE, H. P. PANZER, L. G. MAGLIOCCO and S. A. ASHER, US Pat. 5266 238 (1993).
10. H. P. PANZER, L. G. MAGLIOCCO, M. L. COHEN and W. S. YEN, US Pat. 5338 492 (1994).
11. E. A. KAMENETZKY, L. G. MAGLIOCCO and H. P. PANZER, *Science* **263** (1994) 207.
12. S. A. ASHER, J. HOLTZ, L. LIU and Z. WU, *J. Amer. Chem. Soc.* **116** (1994) 4997.
13. A. S. TSE, Z. WU and S. A. ASHER, *Macromolecules* **28** (1995) 6533.
14. S. A. ASHER, S.-Y. CHANG, S. JAGANNATHAN, R. KESAVAMOORTHY and G. PAN, US Pat. 5452 123 (1995).
15. H. B. SUNKARA, J. M. JETHMALANI and W. T. FORD, *J. Polym. Sci. Part A*; *Polym. Chem.* **32** (1994) 1431.
16. R. S. CRANDALL and R. WILLIAMS, *Science* **198** (1977) 293.
17. R. KESAVAMOORTHY and A. K. ARORA, *J. Phys. A* **18** (1985) 3389.
18. A. IMHOF, A. VAN BLAADEREN and J. K. G. DHONT, *Langmuir* **10** (1994) 3477.
19. M. TOMITA and T. G. M. VAN DE VEN, *J. Phys. Chem.* **89** (1985) 1291.
20. P. A. RUNDQUIST, R. KESAVAMOORTHY, S. JAGANNATHAN and S. A. ASHER, *J. Chem. Phys.* **95** (1991) 8546.
21. P. A. RUNDQUIST, S. JAGANNATHAN, R. KESAVAMOORTHY, C. BRNARDIC, S. XU and S. A. ASHER, *ibid.* **94** (1991) 711.
22. M. S. MALCUIT and C. J. HERBERT, *Acta Physica Polonica A* **86** (1994) 127.
23. C. J. HERBERT and M. S. MALCUIT, *Optics Lett.* **18** (1993) 1783.
24. A. P. PHILIPSE and A. VRIJ, *J. Chem. Phys.* **88** (1988) 6459.
25. J. S. TURNER, "Buoyancy Effects in Fluids" (Cambridge University Press, Cambridge, 1973).
26. V. B. LEONTJEV, SD. D. ABDURAKHMANOV and M. G. LEVKOVICH, in "Proceedings of AIAA/IKI Microgravity Science Symposium" edited by H. C. Gates, Moscow, May 1991 (American Institute of Aeronautics and Astronautics, Washington DC) p. 273.
27. T. P. LYUBIMOVA, in "Reviewed Proceedings of the First International Symposium on Hydromechanics and Heat/Mass Transfer in Microgravity" edited by V. S. Avduesky *et al.* (Gordon and Breach Science, UK, 1992) p. 387.
28. D. STURN, R. MULLER and H.-J. RATH, in "Proceedings of VIIIth European Symposium on Materials and Fluid Science in Microgravity", Vol. 2 (1992) p. 895.
29. M. S. PALEY and D. O. FRAZIER, in "SPIE Space Processing of Materials" edited by N. Ramachandran, Vol. 2809 (International Society of Optical Engineering, Bellingham, 1996) p. 114.
30. D. O. FRAZIER, R. J. HUNG, M. S. PALEY and Y. T. LONG, *J. Crystal Growth* **173** (1997) 172.
31. M. A. NAYLOR and F. W. BILLMEYER Jr, *J. Amer. Chem. Soc.* **75** (1953) 2181.
32. R. W. BUSH, A. D. KETLEY, C. R. MORGAN and D. G. WHITT, *J. Radiat. Curing* **7** (1980) 20.
33. H. C. VAN DE HULST, "Light Scattering by Small Particles" (John Wiley & Sons, New York, 1957).
34. G. OSTER and N-L. YANG, *Chem. Rev.* **68** (1968) 125.
35. D. M. E. THIES-WEESIE and A. P. PHILIPSE, *Langmuir* **11** (1995) 4180.
36. J. A. POJMAN and I. R. EPSTEIN, *J. Phys. Chem.* **94** (1990) 4966.
37. J. A. POJMAN, I. P. NAGY and C. SALTER, *J. Amer. Chem. Soc.* **115** (1993) 11044.
38. R. K. KHANNA and J. SOBHANADRI, *J. Chem. Soc. Farad. Trans.* 2 **70** (1974) 344.
39. R. W. GALLANT and C. L. YAWS, "Physical Properties of Hydrocarbons", Vol. 2, 3rd Edn (Gulf Publishing Company, 1993) p. 76.
40. J. BRANDRUP and E. H. IMMERGUT, "Polymer Handbook", 3rd Edn (John Wiley, New York, 1989) p. V77.
41. "Scientific Polymer Product catalogue".
42. D. R. LIDE (Ed) "CRC Handbook of Chemistry and Physics" (CRC Press, Boca Raton, 1994).

Received 1 May
and accepted 25 September 1997